Theoretical phase diagram of ultrathin films of incipient ferroelectrics

A. R. Akbarzadeh[1,2], L. Bellaiche[2], Jorge Íñiguez[3], and David Vanderbilt[4]
[1]*Department of Materials Science and Engineering, University of California, Los Angeles, P.O. Box 951595, Los Angeles, California 90095-1595, USA*
[2]*Physics Department, University of Arkansas, Fayetteville, AR 72701, Arkansas, USA*
[3]*Institut de Ciencia de Materials de Barcelona (ICMAB-CSIC), Campus UAB, 08193 Bellaterra, Spain and*
[4]*Department of Physics and Astronomy, Rutgers University, Piscataway, New Jersey 08854-8019, USA*
(Dated: February 12, 2007)

We have used a first-principles-based scheme to compute the temperature-versus-misfit strain "Pertsev" phase diagram of ultrathin films of *incipient* ferroelectric $KTaO_3$. Our results suggest that, at variance with the bulk material, $KTaO_3$ ultrathin films cannot be described as quantum paraelectrics. Rather, the behavior of the films is largely determined by surface/interface effects that favor ferroelectricity and the imperfect screening of the depolarizing fields. This leads to Pertsev phase diagrams that are qualitatively similar to those of *normal* ferroelectrics such as $BaTiO_3$.

PACS numbers: 68.55.-a,77.22.Ej,77.80.Bh,77.84.Dy,81.30.Dz

The need for miniaturized devices and the quest for knowledge in nanoscience have led to a flurry of activities in ferroelectric thin films that deepened our understanding of such low-dimensional systems (see Refs. 1, 2, 3 and references therein). In particular, the crucial influence of surface/interface effects and mechanical and electrical boundary conditions on the properties of ferroelectric thin films is now well documented. For instance, recent studies revealed that the strain arising from the substrate can lead to ferroelectric phases absent in the bulk [4, 5, 6] and that surface/interface effects can yield an asymmetric temperature-versus-misfit strain diagram [4, 7]. Similarly, residual depolarizing fields are now known to generate anomalous effects in ferroelectric ultrathin films, such as the existence of stripe domains with remarkably small periods [8, 9, 10].

An important issue that remains to be fully understood concerns the properties of ferroelectric films made of the so-called incipient ferroelectrics, i.e., materials such as $SrTiO_3$ and $KTaO_3$ for which the bulk phase ferroelectricity is suppressed by quantum fluctuations [11, 12, 13]. The pioneering work in Ref. 14 revealed the existence of room-temperature ferroelectricity in strained 500 Å-thick $SrTiO_3$ films, and can thus be taken to suggest that the coupling between strain and dipoles tends to prevail over quantum effects in nanostructures. One may thus wonder what the effect (if any) of quantum zero-point vibrations is in ultrathin films made of incipient ferroelectrics. In particular, the following questions are, to the best of our knowledge, currently unanswered: (1) Can quantum fluctuations overcome the coupling between strain and dipoles in epitaxially *strained* films and, for example, suppress some phases? If so, which phases? (2) For zero misfit strain, are the films paraelectric or ferroelectric? (3) What does the coexistence of quantum and surface/interface effects lead to? (4) What are the consequences and signatures of the zero-point motion of the ions in a film experiencing a depolarizing field?

The aim of this Letter is to answer these questions by determining and analyzing the temperature-versus-misfit strain phase diagrams of $KTaO_3$ ultrathin films under different electrical boundary conditions, using effective models of the films derived from first-principles. As we will see, many interesting features will be revealed and explained.

First-principles-based effective Hamiltonian methods have been very fruitfully employed to study ferroelectric thin films before (see, e.g., Refs. 4, 9, 10, and 15). Here we used such an approach to study $KTaO_3$ ultrathin films grown along the [001] pseudo-cubic direction (chosen to be along the z-axis), having K-O terminated surfaces/interfaces, and being 28 Å thick. Technically, the films are modeled by $10\times10\times7$ supercells that are periodic along the x- and y-axes (which lie along the [100] and [010] pseudo-cubic directions, respectively) and contain seven TaO_2 (001) layers stacked along the non-periodic z-axis. The total energy of such a supercell is written as

$$\mathcal{E}_{\rm tot} = \mathcal{E}_{\rm Heff}(\mathbf{u}_{\rm i}, \mathbf{v}_{\rm i}, \eta) + \beta \mathbf{E}_{\rm d} \cdot \sum_{\rm i} Z^* \mathbf{u}_{\rm i} \ , \qquad (1)$$

where $\mathbf{u}_{\rm i}$ is the local soft mode in the unit cell i of the film, such that $Z^*\mathbf{u}_{\rm i}$ yields the local electrical dipole, and $\beta\mathbf{E}_{\rm d}$ is a term related to screening of the depolarization field, as discussed below. The $\{\mathbf{v}_{\rm i}\}$'s variables describe inhomogeneous strains within the supercell [16]. η is the homogeneous strain tensor, which is particularly relevant to mechanical boundary conditions since epitaxial (001) films are associated with the freezing of some components of η (in Voigt notation), i.e., $\eta_6 = 0$ and $\eta_1 = \eta_2 = \delta$, with δ being the value forcing the film to adopt the in-plane lattice constant of the substrate [5, 6, 9]. In practice, $\delta = (a_{\rm sub} - a_{\rm KTa})/a_{\rm KTa}$, where $a_{\rm sub}$ is the in-plane lattice parameter of the substrate and $a_{\rm KTa} = 3.983$ Å is the 0 K cubic lattice constant of bulk $KTaO_3$ used in Ref. 12.

The expression for $\mathcal{E}_{\rm Heff}$, the intrinsic effective-Hamiltonian energy of the film, is given in Ref. 16. The

first-principles-derived parameters for bulk $KTaO_3$ are those of Ref. 12, except that here we use the formula for the dipole-dipole interactions for thin films under ideal open-circuit (OC) boundary conditions derived in Refs. 17 and 18. Such electrical boundary conditions naturally lead to the existence of a maximum depolarizing field inside the film (denoted by $\mathbf{E}_\mathrm{d}$) when the dipoles all point along the [001] direction. The second term of Eq. (1) mimics a screening of $\mathbf{E}_\mathrm{d}$ via the parameter β. More precisely, the residual depolarizing field resulting from the combination of the first and second terms of Eq. (1) has a magnitude equal to $(1-\beta)\,\mathbf{E}_\mathrm{d}$. As a result, $\beta=0$ corresponds to ideal OC conditions, an increase β lowers the magnitude of the resulting depolarizing field, and $\beta=1$ corresponds to ideal short-circuit (SC) conditions for which the depolarizing field vanishes. Note that $\mathbf{E}_\mathrm{d}$ depends on the dipole configuration, is exactly derived at an atomistic level (following the procedure introduced in Ref. 17), and is self-consistently updated during the simulations.

We should note here the main approximations made in the construction of the above described model for ultrathin films of $KTaO_3$ under varying electrical and mechanical boundary conditions. Firstly, as in previous works [4, 15], our $\mathcal{E}_\mathrm{tot}$ relies on a simple truncation, at the surface/interface layers, of the interactions existing in bulk $KTaO_3$. While this approximation is admittedly crude, the resulting $\mathcal{E}_\mathrm{tot}$ mimics in a qualitatively correct way the enhancement of the surface/interface polar modes that occurs in the most promising compounds (see, e.g., the experimental work on $Ba_{0.5}Sr_{0.5}TiO_3$ films in Ref. 7 or the *ab initio* results for $PbTiO_3$ films sandwiched by Pt electrodes in Ref. 19). In our simple model, such an enhancement happens because our truncation removes short-range interactions that oppose the onset of such local dipoles. At a quantitative level, this approximation may well be underestimating the enhancement for some choices of electrodes and overestimating it for others. At any rate, as the interesting effects resulting from our simulations are very pronounced, we are confident they can be taken as reliable qualitative predictions.

Secondly, we made calculations for ideal electrodes leading to SC boundary conditons (i.e., $\beta=1$), and also for realistic situations for which an appropriate different value of β must be chosen. Let us mention two pieces of information to justify such a choice: (i) the *ab intio* studies of Sai *et al.* [19], who found a 97 % cancellation of the depolarizing field in some systems, and (ii) ongoing unpublished work of one of our co-authors (L. Bellaiche) who, by comparing measurement and simulations, has estimated that some experimental set-ups correspond to a screening of about 98 % of the maximum depolarizing field. Here, we made a conservative choice and used $\beta=0.96$. We thus expect the striking effects predicted will be robust as far as this approximation is concerned.

As in Ref. 12, $\mathcal{E}_\mathrm{tot}$ is used in two different kinds of Monte-Carlo (MC) simulations: classical Monte Carlo (CMC) [20], which does not take into account zero-point vibrations, and path-integral quantum Monte Carlo (PI-QMC) [21, 22, 23], which includes the quantum-mechanical zero-point motions. Consequently, comparing the results of these two different Monte-Carlo techniques allows a precise determination of quantum effects on properties of the considered $KTaO_3$ ultrathin films. We typically used 30,000 MC sweeps to thermalize the system and 70,000 more to compute averages, except at low temperature in PI-QMC where more statistics are needed. Further details about the PI-QMC technique may be found in Refs. 12, 22, and 23.

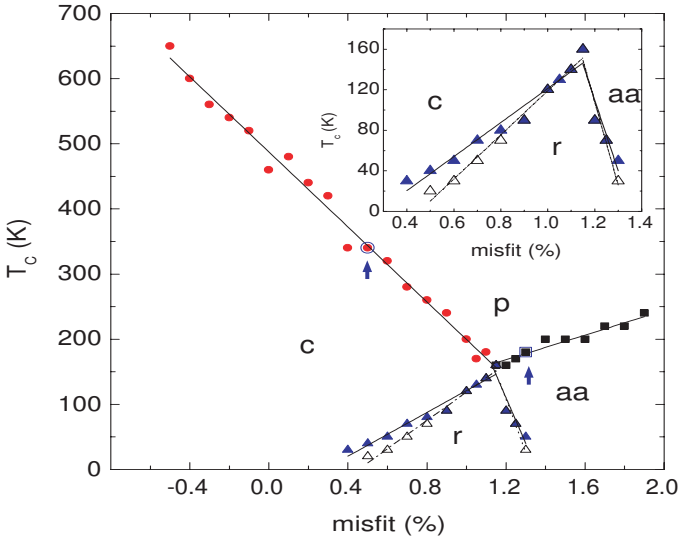

FIG. 1: Temperature *versus* misfit strain diagram of a 28 Å-thick $KTaO_3$ ultrathin film under ideal SC conditions ($\beta=1$). Solid and open symbols refer to CMC and PI-QMC simulations, respectively. Serving as guides for the eyes, the solid and dashed lines are linear fits of the CMC and PI-QMC data, respectively. The inset shows a magnified view of the region in which the *r* phase occurs.

Figure 1 displays the "Pertsev" (that is, the temperature *versus* misfit strain δ) phase diagram for the 28 Å-thick $KTaO_3$ thin film under ideal SC conditions, as resulting from CMC (solid symbols) and PI-QMC (open symbols) simulations. One can clearly see that both kinds of simulations generate the four phases that also appear in the Pertsev diagram of (001) $BaTiO_3$ ultrathin films [4, 6]. These phases are: a paraelectric *p* state at high temperatures; a ferroelectric tetragonal *c* phase for intermediate temperatures and compressive and weakly tensile strains, having a polarization lying along the [001] growth direction; a ferroelectric orthorhombic *aa* phase for low temperatures and large tensile strains, in which the polarization is parallel to the in-plane [110] direction; and a ferroelectric monoclinic *r* phase for the lowest temperatures and intermediate tensile strains, for which the polarization direction continuously rotates from [001] to

[110] as δ increases.

Figure 1 further displays four remarkable features. (1) Quantum effects begin to appear at temperatures below $\approx 100\,\mathrm{K}$ (we numerically found that the transition lines predicted by CMC and PI-QMC overlap above 100 K), as in bullk $KTaO_3$ [12]. As a result, and as emphasized by the inset of the figure, the *c*–to–*r* and, to a lesser extent, the *aa*–to–*r* phase boundaries are the *only* boundaries affected by quantum fluctuations (PI-QMC simulations performed at temperatures higher than 100 K, at 0.5 % and 1.3 % misfit tensile strains, are indicated with arrows in Fig. 1, and reveal that the high-temperature *p*–to-*c* and *p*–to-*aa* phase transitions are unaffected by quantum fluctuations). The effects are, in any case, minor. Essentially, there is a small reduction of the strain range in which the *r* phase occurs: in the low-temperature limit, it passes from about $+0.4\,\% \leq \delta \leq +1.3\,\%$ at a classical level to about $+0.5\,\% \leq \delta \leq +1.3\,\%$ when quantum fluctuations are included. (2) As in $BaTiO_3$ ultrathin films [4, 6], the *p*, *c*, *aa*, and *r* phases *meet* at a single four-phase point, which occurs here at a temperature of about 160 K and a *tensile* strain of about 1.12 % for both CMC and PI-QMC simulations [24]. (3) The phase diagram is asymmetric with respect to zero misfit strain. Such an asymmetry is hinted in experiments on $Ba_{0.5}Sr_{0.5}TiO_3$ films [7] and is related to the enhancement of the z-component of the local dipoles at the surfaces/interfaces. As mentioned above, in our simulations the enhancement occurs because the polar local modes at the surfaces/interfaces are partly free from energetically-costly short-range interactions [25]. (4) For zero misfit strain, the paraelectric–to–*c* transition occurs at about 460 K for both CMC and PI-QMC simulations.

The high transition temperature (T_C) obtained for the film at zero misfit strain starkly contrasts with the behavior the bulk material, for which the paraelectric–to–ferroelectric transition occurs at about 30 K at a classical level and vanishes when quantum effects are considered [12]. The physical origin of such a high T_C lies on the above mentioned dipole enhancement at the surface/interface of the films. The striking consequence of such an enhancement is that these ultrathin films are no longer incipient ferroelectrics, but display a Pertsev phase diagram that is in essence identical to that of a normal ferroelectric like $BaTiO_3$.

It is also interesting to realize that $SrTiO_3$ has a lattice constant about 2 % smaller than $KTaO_3$, and that a linear extrapolation of the data in Fig. 1 suggests that growing $KTaO_3$ ultrathin films on a $SrTiO_3$ substrate (for which $\delta = -2\,\%$) should lead to a T_C that could be as high as 1000 K. In other words, our simulations suggest that growing an ultrathin film made of an incipient material (that is, $KTaO_3$) on a substrate made from another incipient ferroelectric (namely, $SrTiO_3$) may result in a ferroelectric compound with a high T_C and, thus, a large polarization *along the growth direction* at low temperatures. This would be the result of, not only surface/interface effects, but also the well-known coupling between dipoles and compressive strain [26, 27, 28].

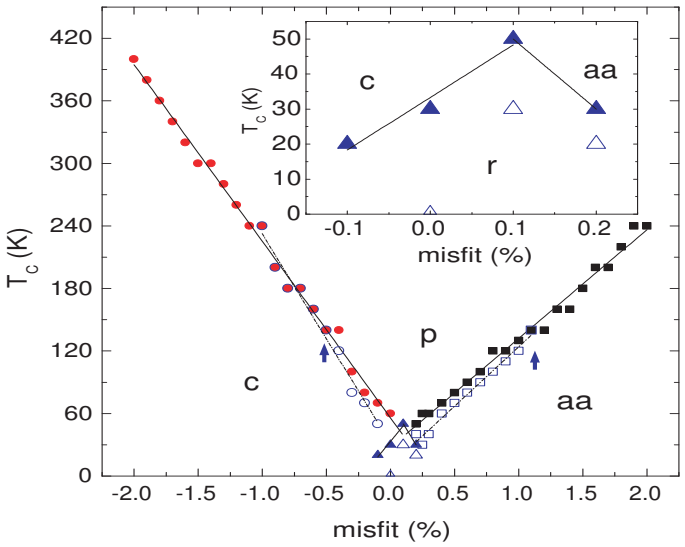

FIG. 2: Temperature *versus* misfit strain diagram of a 28 Å-thick ultrathin film $KTaO_3$ under a residual depolarizing field (β=0.96). Solid and open symbols refer to CMC and PI-QMC simulations, respectively. The solid and dashed lines are linear fits of the CMC and PI-QMC data, respectively, and are guides for the eyes. The inset is a magnification of the region in which the *r* phase occurs, with the PI-QMC data point for the *c*–to–*r* transition temperature at zero misfit strain being a guess resulting from the interpolation of the PI-QMC simulations for the lowest computed temperatures.

We now discuss how depolarizing fields, always present in reality as, e.g., the metallic electrodes are never ideal [29], affect the Pertsev phase diagram of $KTaO_3$ ultrathin films. As explained above, we have chosen $\beta = 0.96$ in Eq. (1), i.e., a situation that corresponds to a screening of 96 % of the maximum depolarizing field. The resulting Pertsev diagram is shown in Fig. 2, for both CMC and PI-QMC simulations. By comparing the CMC results from Figs. 1 and 2, it is clear that the depolarizing field tends to suppress the z-component of the polarization, as expected. Indeed, this effect dramatically decreases the *p*–to–*c* transition temperatures; for instance, the transition occurs around 60 K at zero misfit strain, i.e., the T_C is 400 K lower than the one obtained for ideal SC. It also considerably extends the region of small tensile strain associated with the *aa* phase, which exhibits an in-plane polarization that does not directly feel the depolarizing field, and significantly narrows the *r-phase* region.

As a result, the phase diagram becomes more symmetric around the zero misfit strain and the four-phase point of Fig. 1 shifts towards lower temperature (about 50 K for CMC simulations [24]). As shown in Fig. 2, such a small transition temperature implies that the quantum fluctuations (which are appreciable only at temperatures

below 120 K, and become more pronounced as the temperature decreases) have two remarkable effects that do *not* occur in the film under SC conditions. First of all, the zero-point vibrations now affect the p–to–c and p–to–aa phase boundaries (for small strain) – in addition to the boundaries involving the r phase. Secondly, quantum fluctuations significantly reduce the stability range of the *r-phase*. This suggests that, for slightly worse electrodes (i.e., for $\beta < 0.96$), quantum effects could well lead to the disappearance of the four-phase point in favor of a *three*-phase point in which "only" the p, c, and aa meet.

In summary, we have used a first-principles-based scheme to determine the temperature-versus-misfit strain "Pertsev" phase diagram of ultrathin films of *incipient* ferroelectric $KTaO_3$ under short-circuit-like boundary conditions. We have performed both classical and quantum Monte Carlo simulations, the ionic quantum fluctuations being fully taken into account in the latter. This has allowed us to investigate the competition of the various effects present in the films, namely, the misfit strains and surface/interface effects that are known to favor the occurrence of ferroelectric phases, and the zero-point vibrations and residual depolarizing fields that tend to suppress ferroelectricity.

We have found that, for ideal electrodes, quantum fluctuations have a negligible effect; the phase diagram is essentially determined by the other factors mentioned above and closely resembles what is found in, e.g., $BaTiO_3$ films. Our results thus suggest that, in ultrathin film form, *quantum paraelectrics* such as $KTaO_3$ behave qualitatively in the same way as *strong* ferroelectrics such as $BaTiO_3$. We have also simulated realistic (thus imperfect) electrodes and found that the corresponding depolarizing fields have a great impact on the calculated phase diagram; in particular, the transition temperatures of the c and r phases are significantly reduced. As a result, quantum mechanical effects become more important in this case, and may alter the phase diagram qualitatively, e.g., by suppressing the r phase.

We believe the present study leads to a better understanding of ferroelectric thin films, and hope it will stimulate experimental work aimed at confirming our predictions.

We thank George A. Samara and Kevin Leung for useful discussions. This work is supported by ONR grants N00014-01-1-0365, N00014-04-1-0413, and N00014-05-1-0054, by NSF grant DMR-0404335, and by DOE grant DE-FG02-05ER46188. J.I. thanks support from the Spanish Ministry of Science and Education (FIS2006-12117-C04-01) and FAME-NoE.

[1] M. Dawber, K. M. Rabe, and J. F. Scott , Rev. Mod. Phys. **77** 1083, (2006).
[2] J. F. Scott, Science **246**, 1400 (1989).
[3] I. Kornev, H. Fu and L. Bellaiche, J. Mater. Sci. **41**, 137 (2006).
[4] B.-K. Lai, I. Kornev, L. Bellaiche, and G. J. Salamo, Appl. Phys. Lett. **86**, 132904 (2005).
[5] N. A. Pertsev, V. G. Kukhar, H. Kohlstedt and R. Waser, Phys. Rev. B **67**, 054107 (2003).
[6] O. Diéguez et al., Phys. Rev. B **69**, 212101 (2004).
[7] S. Rios, J. F. Scott, A. Lookman, J. McAneney, R. M. Bowman, and J. M. Gregg, J. Appl. Phys. **99**, 024107 (2006).
[8] S. K. Streiffer et al., Phys. Rev. Lett. **89**, 067601 (2002).
[9] I. Kornev, H. Fu and L. Bellaiche, Phys. Rev. Lett. **93**, 196104 (2004).
[10] I. Ponomareva and L. Bellaiche, Phys. Rev. B **74**, 064102 (2006).
[11] R. Viana, P. Lunkenheimer, J. Hemberger, R. Bohmer, and A. Loidl, Phys. Rev. B **50**, 601(R) (1994).
[12] A. R. Akbarzadeh, L. Bellaiche, K. Leung, J. Iniguez, and David Vanderbilt, Phys. Rev. B **70**, 054103 (2004).
[13] B. Salce, J. L. Gravil, and L. A. Boatner, J. Phys.: Condens. Matter **6**, 4077 (1994).
[14] J. H. Haeni et al., Nature **430**, 758 (2004).
[15] P. Ghosez and K. M. Rabe, App. Phys. Lett. **76**, 2767 (2000).
[16] W. Zhong, D. Vanderbilt and K.M. Rabe, Phys. Rev. Lett. **73**, 1861 (1994); Phys. Rev. B **52**, 6301 (1995).
[17] I. Ponomareva, I. Naumov, I. Kornev, H. Fu and L. Bellaiche, Phys. Rev. B **72**, 140102 (R) (2005).
[18] I. I. Naumov and H. Fu, cond-mat/0505497 (2005).
[19] N. Sai, A. M. Kolpak, and A. M. Rappe, Phys. Rev. B **72**, 020101(R) (2005).
[20] N. Metropolis, A. W. Rosenbluth, M. N. Rosenbluth, A. H. Teller, and E. Teller, J. Chem. **21**, 1087 (1953).
[21] W. Zhong and D. Vanderbilt, Phys. Rev. B **53**, 5047 (1996).
[22] J. Íñiguez and D. Vanderbilt, Phys. Rev. Lett. **89**, 115503 (2002).
[23] D. M. Ceperley, Rev. Mod. Phys. **67**, 279 (1995).
[24] Note that the lines displayed in Figs. 1 and 2 do not intersect at an accurately defined strain-temperature four-phase point. This is partly because the transition lines are *linear* fits of our simulated data points, and also because we have a 10 to 20 K uncertainty in the predicted transition temperatures.
[25] For zero misfit strain, $\beta = 1$, and $T = 50$ K, both CMC and PI-QMC rendered $u_z \approx 0.041$ and 0.037 a.u. for surface/interface and inner layers, respectively. For $\beta = 0.96$, these values get reduced to 0.015 and 0.013 a.u., respectively, for CMC, and to 0.013 and 0.012 a.u., respectively, for PI-QMC. The corresponding magnitude of the local mode is 0.024 a.u. at $T = 20$ K in bulk $KTaO_3$, according to CMC.
[26] N. A. Pertsev, A. K. Tagantsev, and N. Setter, Phys. Rev. B **61**, 825 (R) (2000).
[27] R. D. King-Smith, and D. Vanderbilt, Phys. Rev. B **49**, 5828 (1994).
[28] R. E. Cohen, Nature **358**, 136 (1992).
[29] J. Junquera and P. Ghosez, Nature **422**, 506 (2003).